Nuclear Instruments and Methods in Physics Research B 393 (2017) 17–21

Contents lists available at ScienceDirect

Nuclear Instruments and Methods in Physics Research B

journal homepage: www.elsevier.com/locate/nimb

Simple model of surface roughness for binary collision sputtering simulations

Sloan J. Lindsey [a], Gerhard Hobler [a,*], Dawid Maciążek [b], Zbigniew Postawa [b]

[a] Institute of Solid-State Electronics, TU Wien, Floragasse 7, A-1040 Wien, Austria
[b] Institute of Physics, Jagiellonian University, ul. Lojasiewicza 11, 30348 Kraków, Poland

ARTICLE INFO

Article history:
Received 19 July 2016
Received in revised form 16 September 2016
Accepted 29 September 2016
Available online 7 October 2016

Keywords:
Sputtering
Surface roughness
Binary collision simulations
Molecular dynamics

ABSTRACT

It has been shown that surface roughness can strongly influence the sputtering yield – especially at glancing incidence angles where the inclusion of surface roughness leads to an increase in sputtering yields. In this work, we propose a simple one-parameter model (the "density gradient model") which imitates surface roughness effects. In the model, the target's atomic density is assumed to vary linearly between the actual material density and zero. The layer width is the sole model parameter. The model has been implemented in the binary collision simulator IMSIL and has been evaluated against various geometric surface models for 5 keV Ga ions impinging an amorphous Si target. To aid the construction of a realistic rough surface topography, we have performed MD simulations of sequential 5 keV Ga impacts on an initially crystalline Si target. We show that our new model effectively reproduces the sputtering yield, with only minor variations in the energy and angular distributions of sputtered particles. The success of the density gradient model is attributed to a reduction of the reflection coefficient – leading to increased sputtering yields, similar in effect to surface roughness.

1. Introduction

It is well known that ion bombardment roughens the target surface [1], which in turn may influence the sputtering yield [2]. In a recent study [3] we demonstrated that the simulation of sputtering yields for grazingly incident ions requires the consideration of surface roughness. Grazing incidence conditions are typically found during transmission electron microscopy (TEM) sample preparation, one of the most important applications of focused ion beams (FIB) [4,5]. Glancing incidence angles may also occur during FIB milling of holes [6] or during irradiation of nanowires, for instance, when the nanowires bend towards the beam [7]. Recently, several groups have developed Monte Carlo binary collision (BC) codes that are capable of simulating ion bombardment of 2D and 3D micro- and nanostructures [8–14]. They all lack models of surface roughness, prohibiting meaningful simulation of glancing angle effects.

BC simulation studies of the effect of surface roughness on sputtering have mostly used geometrically modified flat surfaces, employing square waves [2], sinusoidal waves [3], or by applying fractal surface models [15,16]. All these models would be difficult to implement in 2D and 3D simulations, since the simulation needs to store a rough surface geometry interspersed with any mesoscale topographies of interest.

Yamamura et al. [2] have shown that reducing the target density in a surface layer has a similar effect as a geometrically defined rough surface. However, they used a monoatomic surface layer only, which limited the degree of roughness that could be introduced. In the present work, we generalize Yamamura's idea by using a surface layer with a density that decreases linearly towards the surface, which we henceforth call density gradient model. The sole parameter of this model is the thickness of the layer, which may be larger than monoatomic. This removes ambiguity from the model as compared to, e.g., the sinusoidal model where fits to the experimental data are available across multiple pairings of wavelengths and amplitudes [3]. Equally important, the density gradient model is easily implemented in 2D and 3D BC simulations.

To validate the model, we compare sputtering yields and energy and angular distributions of sputtered atoms with the predictions of three geometrically defined models with wave vectors parallel to the projection of the ions' incidence direction to the surface. To aid the construction of a realistic rough surface, we have also performed molecular dynamics (MD) simulations of sequential Ga impacts on a Si surface.

This study is carried out for 5 keV Ga ions impinging on Si. The simulations are compared to experimental data obtained at FEI

* Corresponding author.
E-mail address: gerhard.hobler@tuwien.ac.at (G. Hobler).

http://dx.doi.org/10.1016/j.nimb.2016.09.028
0168-583X/

Company [17]. A lower ion energy is used than in our previous study [3] mainly to facilitate the MD simulations.

2. Simulation specifics

2.1. MD modeling

MD modeling was carried out at Jagiellonian University using a modified version of LAMMPS [18]. The simulation cell was 120 Å × 120 Å × 80 Å initially filled with single-crystalline (100)-Si with a (2 × 1) reconstructed surface. The number of Si atoms in this cell was 57112. Periodic boundary conditions were used in the lateral directions. Stochastic and rigid layers, 7 Å and 3 Å thick, respectively, were used at the bottom to simulate the thermal bath that kept the sample at the required temperature and to keep the shape of the sample. The simulations were run at 0 K temperature. The target was sequentially bombarded with 5 keV Ga ions at polar angles of 89° and 85° and an azimuthal angle of 35° with respect to the cell edge which is a [010] direction. The latter was chosen as to minimize possible artifacts of the periodic boundary conditions due to the passage of the ions over regions they have previously interacted with while slowly glancing off the surface. Each impact was simulated for 2 ps. The resulting structure was used as initial condition for the subsequent impact after removal of all sputtered atoms and any excess kinetic energy from the system. The latter was achieved by an energy quenching procedure that involved application of gentle viscous damping forces to the entire sample for 0.2 ps. A Tersoff-3 potential [19] was used for Si-Si interactions, and the ZBL potential [20] splined with a Lennard-Jones (LJ) potential for Ga-Si interactions.

2.2. BC modeling

Monte Carlo simulations using the BC approximation were carried out at TU Wien using the simulator IMSIL [21,22]. As in our earlier work [3] we use the ZBL interatomic potential [20], the Oen– Robinson model for electronic stopping [23] with a cutoff energy of 10 eV, and a planar surface potential with a surface binding energy between Si and Si of 4.7 eV. Since the refraction of the incident ions at the surface potential is significant under the conditions studied, the choice of the surface binding energy between Ga and Si is also critical. We use a value of 2.82 eV [24]. All of the BC simulations were carried out using the static mode of IMSIL, wherein the target starts in an amorphous state as pure silicon, and its modification by the implanted gallium is not taken into account over the course of the simulation. 25,000 impacts were carried out for sputter yield calculations and 5 million impacts for determining the energy and angular distributions of sputtered atoms.

2D geometries are specified in IMSIL by polygons which are converted to a signed distance function defined on a Cartesian grid covering the simulation domain [13]. IMSIL was adapted for this research through the addition of a periodic geometry mode, which allowed to set the lateral size of the simulation domain equal to one wavelength. The vertical size was chosen 300 Å plus the roughness amplitude, which led to a negligible forward sputtering yield of 2×10^{-4}, thus indicating sufficient thickness to simulate an infinitely thick target. In order to exclude any significant discretization errors, we used 2000 segments for the polygons and 1 million cells for the internal grid.

Three geometric surface models were used: Cosine, triangular, and double cosine (Fig.1). The double cosine function is defined by the superposition of two cosine functions with wavelengths differing by a factor of three:

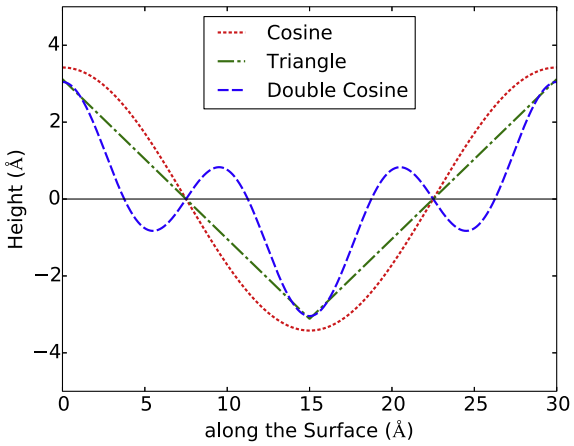

Fig. 1. Geometric roughness models used in this study, shown for a wavelength of 30 Å: Cosine, triangular, and double cosine. All surface models are shown with best-fit parameters.

$$z(x) = \frac{A}{2}\left(\cos\frac{2\pi}{\lambda}x + \cos\frac{6\pi}{\lambda}x\right), \tag{1}$$

where A is the amplitude and λ is the period. The choice of the wavelength λ is not very critical and will be estimated from the results of the MD simulations. The amplitude A will be determined by fitting to experimental sputtering yield data.

The density gradient model is implemented by creating collision partners at the end of the free flight paths with probabilities

$$p = \begin{cases} 1 & \text{for } d \geqslant w \\ d/w & \text{for } 0 < d < w \\ 0 & \text{for } d \leqslant 0, \end{cases} \tag{2}$$

where d denotes the signed distance from the surface (negative values outside the target) and w is the width of the density gradient layer. Effectively this means that the density of target atoms decreases linearly towards the surface within the layer $0 < d < w$, as illustrated in Fig. 2a. The parameter w will be determined by fitting to the experimental sputtering yield data. Note that in the limit of zero wavelengths the geometric surface models correspond to reduced-density layers. These densities are shown in Fig. 2b and are compared with the density gradient model.

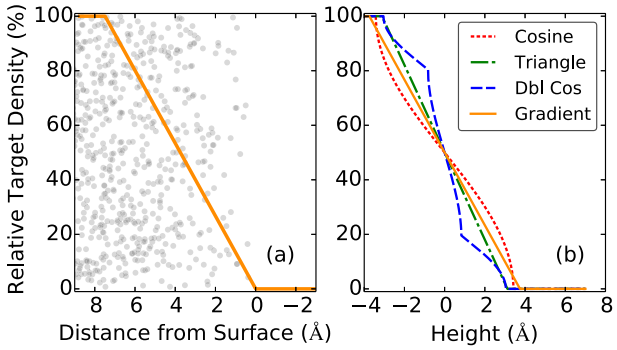

Fig. 2. (a) Schematic drawing of the target density in the density gradient model. Filled circles represent atoms. (b) Comparison of the density with equivalent density profiles of the geometric roughness models. The height axis in (b) has been shifted with respect to (a) so its origin is at the center of each roughness layer. All surface models are shown with best-fit parameters.

3. Results

MD simulations were performed for an incidence angle of 89° with different binding energies of the LJ potential. The best fit to the experimental sputter yield of 1.7 was obtained with a binding energy of 0.9 eV. In these simulations, the sputtering yield was averaged between the 1100th impact, when the sputtering yield had stabilized, and the 2191st (last) impact. With the same binding energy, impacts at an incidence angle of 85° were simulated resulting in a sputtering yield of 6.49, which compares favorably with the experimental value of 6.66, thus giving confidence in the simulations. The RMS roughness amplitudes of the surface after the last impact are 2.8 Å and 3.1 Å for incidence angles of 89° and 85°, respectively.

Inspection of the surface at the end of the simulation reveals intertrough/intercrest distances of approximately 20–50 Å (Fig. 3). We therefore chose a wavelength of $\lambda = 30$ Å for our geometric roughness models. BC simulations were then performed with all models, and least squares fitting was used to determine the best fit of the amplitudes A to the experimental sputtering yields at incidence angles of 86.6°, 88.1°, and 89°, resulting in $A = 3.42$ Å, 3.12 Å, and 3.04 Å for the cosine, triangle, and double cosine model, respectively. In the same way the best-fit layer width $w = 7.49$ Å of the density gradient model was obtained. The surface models with these optimized parameters are represented in Figs. 1 and 2. Sputtering yields obtained with these models are shown in Fig. 4a and b, and are compared with the experimental data. Good fits are observed for all roughness models. Interestingly, the density gradient model features the best fit (see Fig. 4b). In contrast, large deviations between simulation results and experimental data are observed when a flat surface is assumed in BC simulations of incidence angles larger than ~82°. Comparing this to our earlier study of 30 keV Ga ions impinging on Si [3], where flat surface simulations have been found to deviate from the experimental data at angles larger than ~86°, it may be concluded that the range of conditions at which sputtering yields are affected by surface roughness, increases with decreasing ion energy.

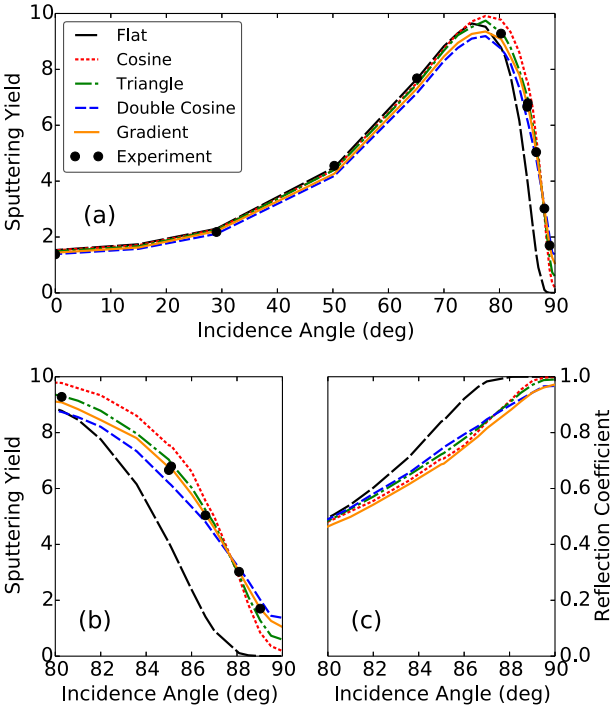

Fig. 4. (a,b) Sputtering yields as a function of incidence angle: Experimental data [17] (filled circles), simulation results for a flat surface (long-dashed line) and for the various roughness models with the amplitude fitted to the last three experimental data points, (b) is a magnification of the range between 80° and 90°, (c) shows the reflection coefficients obtained with all models.

The reflection coefficients (the fraction of the incident ions that are reflected or backscattered) in these simulations are shown as a function of incidence angle in Fig. 4c. The results indicate that all models that include surface roughness increase the sputtering yield by means of reducing the reflectivity of the target. The relation between sputtering yield and reflection coefficient is easily understood, as reflected ions interact weaker with the target and therefore produce fewer recoils than ions that are scattered into the material.

While it is reassuring that the density gradient model fits the experimental sputtering yield data over the whole range of incidence angles with a single value of the layer width, higher order yield statistics such as the energy and angular distribution of the sputtered atoms are also important, especially when the simulation data is used as an input to topography simulations [17,26,27]. Modeling of surface roughness clearly plays a role in the resulting energy and angular distributions as shown in Fig. 5a and b, respectively. For this comparison, energy and angular distributions have been simulated for an incidence angle of 87.7°, the approximate crossover point of the sputtering yield curves obtained with the four roughness models (see Fig. 4b). Near-perfect agreement of the energy distributions is observed between all roughness models, while the energy distribution of atoms sputtered from the flat surface (black long-dashed line) is significantly different. For the angular distribution the agreement between the roughness models is less marked, but all four roughness models yield a more pronounced first-knock-on peak than the flat surface. This peak in the angular distribution is attributed to high-energy ejected target atoms that undergo relatively few collisions before leaving the target and thus retain more energy and a greater fingerprint of the incoming ion trajectory. The larger role of primary recoils in sputtering from a rough surface can also be induced from

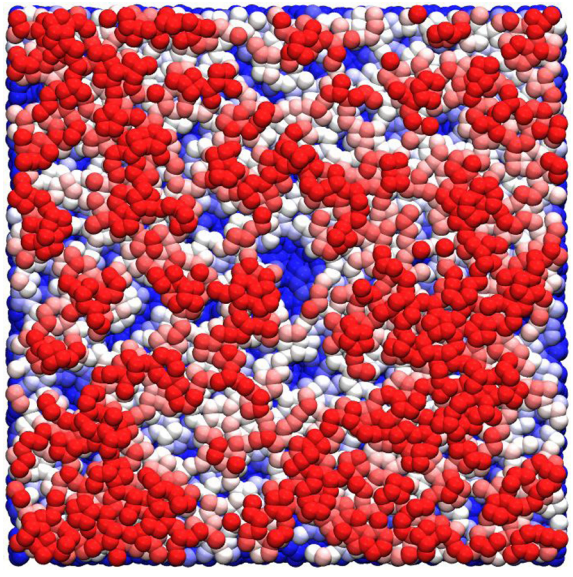

Fig. 3. Top view of the silicon sample after 2100 sequential hits by 5 keV Ga ions simulated by MD for a polar angle of 89° and an azimuthal angle of 35°. Atoms are colored according to their z coordinate; red: the position of the topmost atoms, white: 3 Å below the top level, and blue: 6 Å below the top level. The edge length of the cell shown is 120 Å. (For interpretation of the references to color in this figure legend, the reader is referred to the web version of this article.)

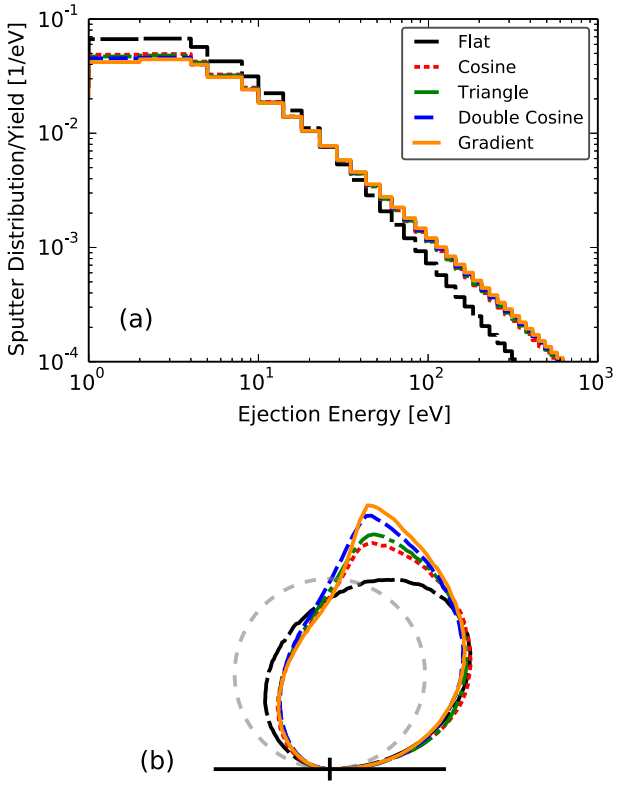

Fig. 5. (a) Energy distributions and (b) angular distributions of sputtered particles obtained by BC simulations at an incidence angle of 87.7°: Flat surface (long-dashed line) compared to the four roughness models. The gray dashed circle in (b) indicates a cosine distribution, which is predicted by theory [25] for well developed cascades.

the energy distribution which is weaker than E^{-2}, since a dependence as E^{-2} is expected when the collision cascades are well developed [25].

Despite the favorable results presented so far, there is one discrepancy: The RMS amplitudes obtained from the MD simulations are larger than those of the geometric roughness models fitted to the experimental data. To shed light on a possible explanation, we have fitted the amplitudes of our three geometric roughness models as a function of the wavelength. The results for the amplitudes are presented in Fig. 6 (upper curves) together with the corresponding RMS values (thinner broken lines in the lower part of the figure). It can be seen that the amplitudes rise towards small wavelengths. This can tentatively be explained by the increasing role of redeposition: With decreasing wavelength the aspect ratio of the topography increases, which increases the amount of redeposition. Redeposited atoms are not sputtered, so to fit the model to the experimental sputtering yield, the roughness amplitude has to be increased. When using a roughness model with a wavelength $\lambda > 10$ Å in the BC simulations, short-wavelength components that are present in the MD simulations are suppressed, therefore redeposition is underestimated, and smaller amplitudes are sufficient to fit the experimental data. It should be noted, however, that other factors may play a role such as the planar surface potential model used in the BC simulations that becomes questionable on a rough surface.

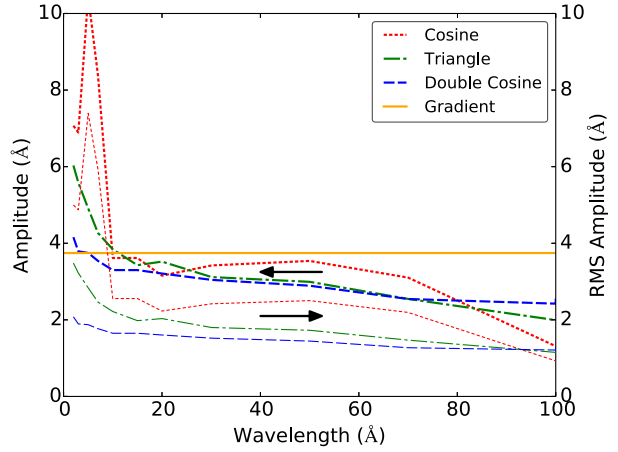

Fig. 6. Best fits of roughness profile amplitudes to the experimental data as a function of assumed wavelength. While the upper three, thicker lines show the amplitude A, the lower three, thinner lines represent the respective RMS values. Half of the best-fit layer thickness w of the density gradient model is shown for comparison (horizontal line labelled "gradient").

We note that all wavelengths except for extremely small ones (~1 Å) give sputtering yields that are in good agreement with the experimental data over the whole range of incidence energies (not shown).

4. Conclusions

We have demonstrated that the newly proposed "density gradient" model can be used to fit BC simulations to experimental data on sputtering yields as a function of incidence angle. We have also shown that a variety of roughness models is capable of describing the data reasonably with the density gradient model providing the best fit in the particular case studied. That one and the same roughness model can describe sputtering conditions for all incidence angles, is not self-evident – different surface roughness could develop as a result of different incidence angles. Our MD simulations show that for 5 keV Ga bombardment of Si the RMS roughness amplitude is only slightly different for incidence angles of 85° and 89°. We have not investigated surface roughness for more-perpendicular ion impact. However, moderate beam-induced surface roughness as investigated in this work, affects sputtering yields only weakly at most incidence angles (<82° for 5 keV Ga incident on Si). So even a discrepancy of the roughness model with the actual target topography at these less-oblique incidence angles would not inhibit successful simulation of sputtering effects.

We have also shown that all roughness models investigated lead to almost identical energy distributions of the sputtered atoms and to similar angular distributions and reflection coefficients. It may be concluded that the main effect of a surface roughness model for sputtering simulations must be a reduction in the reflection coefficient, while the actual shape of the assumed surface is of less importance as long as the correct sputtering yield is fitted. This explains why a physically questionable model – densities approaching zero as in our density gradient model are not possible in condensed matter – may be so successful.

The new density gradient model is computationally efficient and easy to implement in BC codes. This is true even for 2D and 3D topographies, provided a signed distance function field is available such as in our IMSIL simulator. It is hoped that the new roughness model enables a greater degree of realism in BC sputtering simulations with very little computational overhead.

Acknowledgments

MK and ZP would like to gratefully acknowledge financial support from the Polish National Science Center, Program No. 2013/09/B/ST4/00094.

References

[1] E.A. Eklund, R. Bruinsma, J. Rudnick, R.S. Williams, Phys. Rev. Lett. 67 (1991) 1759.
[2] Y. Yamamura, C. Mossner, H. Oechsner, Radiat. Eff. 103 (1987) 25.
[3] S. Lindsey, G. Hobler, Nucl. Instrum. Methods B 303 (2013) 142.
[4] L. Giannuzzi, F. Stevie, Micron 30 (1999) 197.
[5] J. Mayer, L.A. Giannuzzi, T. Kamino, J. Michael, MRS Bull. 32 (2007) 400.
[6] W.C.L. Hopman, F. Ay, W. Hu, V.J. Gadgil, L. Kuipers, M. Pollnau, R.M.D. Ridder, Nanotechnology 18 (2007) 195305.
[7] M. Bettge, S. MacLaren, S. Burdin, R.T. Haasch, D. Abraham, I. Petrov, M.-F. Yu, E. Sammann, Nanotechnology 23 (2012) 175302.
[8] I. Bizyukov, A. Mutzke, R. Schneider, A.M. Gigler, K. Krieger, Nucl. Instrum. Methods B 266 (2008) 1979.
[9] C. Borschel, C. Ronning, Nucl. Instrum. Methods B 269 (2011) 2133.
[10] W. Möller, Nucl. Instrum. Methods B 322 (2014) 23.
[11] R. Timilsina, S. Tan, R. Livengood, P.D. Rack, Nanotechnology 25 (2014) 485704.
[12] G. Hobler, D. Kovac, Nucl. Instrum. Methods B 269 (2011) 1609.
[13] G. Hobler, Nucl. Instrum. Methods B 352 (2015) 22.
[14] Y.G. Li, Y. Yang, M.P. Short, Z.J. Ding, Z. Zeng, J. Li, Sci. Rep. 5 (2015) 18130.
[15] T. Kenmotsu, Y. Yamamura, T. Muramoto, N. Hirotani, Nucl. Instrum. Methods B 228 (2005) 369.
[16] A. Hu, A. Hassanein, Nucl. Instrum. Methods B 281 (2012) 15.
[17] S.J. Lindsey, PhD Thesis, TU Wien, Vienna, Austria, 2015.
[18] S. Plimpton, J. Comput. Phys. 117 (1995) 1.
[19] J. Tersoff, Phys. Rev. B 39 (1989) 5566.
[20] J.F. Ziegler, J.P. Biersack, U. Littmark, The Stopping and Range of Ions in Solids, Pergamon Press, New York, 1985.
[21] G. Hobler, Nucl. Instrum. Methods B 96 (1995) 155.
[22] C. Ebm, G. Hobler, Nucl. Instrum. Methods B 267 (2009) 2987.
[23] O.S. Oen, M.T. Robinson, Nucl. Instrum. Methods 132 (1976) 647.
[24] Y. Kudriavtsev, A. Villegas, A. Godines, R. Asomoza, Appl. Surf. Sci. 239 (2005) 273.
[25] P. Sigmund, Phys. Rev. 184 (1969) 383.
[26] H.-B. Kim, G. Hobler, A. Lugstein, E. Bertagnolli, J. Micromech. Microeng. 17 (2007) 1178.
[27] H.-B. Kim, G. Hobler, A. Steiger, A. Lugstein, E. Bertagnolli, Nanotechnology 18 (2007) 245303.